

Exploration of Wire Array Metamaterials for the Plasma Axion Haloscope

M. Wooten,¹ A. Droster,¹ Al Kenany,^{1,2} D. Sun,¹ S.M. Lewis,¹ and K. van Bibber¹

¹*Department of Nuclear Engineering, University of California Berkeley, Berkeley, CA 94720 USA*

²*Accelerator Technology and Applied Physics Division,
Lawrence Berkeley National Laboratory, Berkeley, CA 94720*

(Dated: March 31, 2022)

A plasma haloscope has recently been proposed as a feasible approach to extend the search for dark matter axions above 10 GHz ($\sim 40 \mu\text{eV}$), whereby the microwave cavity in a conventional axion haloscope is supplanted by a wire array metamaterial. As the plasma frequency of a metamaterial is determined by its unit cell, and is thus a bulk property, a metamaterial resonator of any frequency can be made arbitrarily large, in contrast to a microwave cavity which incurs a steep penalty in volume with increasing frequency. We have investigated the basic properties of wire array metamaterials through S_{21} measurements in the 10 GHz range. Excellent agreement with theoretical models is found, by which we project achievable quality factors to be of order 10^4 in an actual axion search. Furthermore, schemes for tuning the array over a usable dynamic range (30% in frequency) appear practical from an engineering perspective.

INTRODUCTION

The axion, a light pseudoscalar emerging from the Peccei-Quinn mechanism to suppress CP-violating effects in the Strong Interaction [1-3] would also be copiously produced in the early universe, and thus represents an interesting dark matter candidate. The mass of the axion corresponding to the estimated dark matter density of the universe, however is poorly constrained. In cosmological scenarios of long low-scale inflation, the axion mass may be as low as 10^{-12} eV [4,5]. In the case of Peccei-Quinn symmetry breaking after inflation, the mass is much higher, but more significantly is uniquely determined and in principle exactly calculable [6,7]. While calculating the evolution of the axion string network over cosmological time is an extremely challenging problem, recent adaptive mesh refinement simulations represent a major advancement over prior work and now predict the axion mass to be in the range (40-180) μeV with a preferred value of $65 \pm 6 \mu\text{eV}$ [7]; larger simulations will constrain this range more tightly in the near future.

Along with the many orders of magnitude of mass to be searched, the couplings of the axion to radiation and matter are also expected to be extraordinarily weak, making the experimental front extremely challenging as well. The primary strategy for the detection of halo dark matter axions is their conversion to photons in a magnetic field, resonantly enhanced inside a microwave cavity [8,9], although other concepts are under development [10,11]. The predicted conversion power is miniscule for current experiments, $\sim 10^{-(23-24)}$ Watts [12-15], and thus rendering such a signal observable depends on two factors. The first is aggressive noise reduction, where the microwave cavity axion search has been both a driver and beneficiary of advances in quantum metrology [15,16]. The second is maximizing the signal power itself, where the conversion power scales with factors under

the experimenter's control as $P \propto B_0^2 V C Q$, where B_0 is the strength of the magnetic field. The remaining three parameters are properties of the microwave cavity, i.e. the volume V , the quality factor Q , and the form factor C for the operating mode, the latter reflecting the overlap of the mode's E -field with the external magnetic field B_0 . The TM_{010} is generally the mode of choice, as its form factor is usually the largest. The connection between frequency and physical size of a microwave cavity as limited by the magnet bore, is what in fact centers current experiments around the 0.5-5 GHz decade. To reach axions of much lower mass, neV or lower, associated with slow-roll inflation scenarios, variants of the microwave cavity scheme have been proposed whereby the frequency of the resonator is determined by a lumped-element LC circuit external to the conversion volume [17,18]. A pilot experiment based on this concept has been carried out [19], and a full-scale experiment capable of reaching QCD axion models is being actively pursued [20].

For the post-inflation axion, the search will need resonators that can scan up to an order of magnitude higher in frequency than current experiments. The practicality of scaling current cylindrical cavities to this range is limited due to the inherent connection between cavity frequency, volume and Q value which would substantially reduce signal power. Two strategies have been pursued to make a resonator that is simultaneously large volume and high frequency. One is to insert multiple axial metal posts into a single large cavity to raise and tune its frequency [21]. The other is to make an array of multiple small cavities all tuned in concert and combined in phase [22]. But even these are very complex from an engineering standpoint, and are limited to only modest extensions of currently accessible frequency for the microwave cavity axion search.

THE TUNABLE PLASMA HALOSCOPE

Motivated by the need to develop a practical search strategy for the post-inflation axion, Lawson et al. have proposed a radically different approach to decoupling the size and frequency of a resonator by replacing the microwave cavity with a metamaterial serving a surrogate plasma [23]. Whereas the frequency of a cavity mode is determined by its boundary conditions and thus its physical dimensions, for a metamaterial, the plasma frequency is a function of its unit cell, and is thus independent of its physical dimensions. In principle a resonator could be designed to be for all practical purposes both arbitrarily high in frequency and arbitrarily large. This would open up new design options, for example an experiment based on a very large volume, medium-field magnet such as a whole-body MRI scanner, or a collider detector magnet, in contrast to current experiments built on small volume, very high field magnets. Lawson et al. propose a metamaterial of a uniform array of thin parallel wires as a potentially viable solution, for which there is a well-developed theory and some experimental validation [24-26].

As a simple illustrative case, Pendry et al. [24] consider an array of thin wires of radius r in a square lattice of separation a , oriented in the \hat{z} direction, and in an approximate treatment demonstrate that the array supports a longitudinal plasmonic mode, with a plasma frequency given by

$$\nu_p^2 = \frac{c^2}{2\pi a^2 \ln\left(\frac{a}{r}\right)} \quad (1)$$

For $a = 5$ mm and $r = 25$ μm , representative of parameters in our study, the plasma frequency, $\nu_p = 10.75$ GHz. Belov et al. have developed a more accurate analytic result and have also generalized it to rectangular lattices [25],

$$\nu_p^2 = \frac{c^2}{2\pi s^2 \left(\ln\left(\frac{s}{2\pi r}\right) + F(u) \right)} \quad (2a)$$

where $s = \sqrt{ab}$, $u = a/b$, and

$$F(u) = -\frac{1}{2} \ln(u) + \sum_{n=1}^{\infty} \frac{\coth(\pi n u) - 1}{n} + \frac{\pi u}{6} \quad (2b)$$

GOALS AND APPROACH

The substitution of a wire array metamaterial for a microwave cavity is not entirely straightforward; there are features that differ from a cavity resonator that affect the practical considerations in building a metamaterial-based haloscope. These include, for example, the design

of the antenna to couple out power to the receiver. Furthermore, while the plasmon excitation is largely self-contained, the wire array metamaterial itself needs to be shielded by a conducting enclosure, that will need to be incorporated into the microwave simulations of the overall resonator. This paper will be limited just to basic studies of the wire array metamaterial that will determine its fundamental suitability for the haloscope application. These include the dependence of its properties as a function of its size, some estimate of Q that may be achievable in situ, and how the array could be tuned over a usable dynamic range.

Measurement of the microwave transmission, i.e. the S_{21} parameter is an accurate and reliable tool for determining the properties of a complex dielectric, which has been previously applied in early studies of wire array metamaterials [24,26]. Furthermore, particularly to study the evolution of metamaterial behavior as a function of spatial extent, it was natural and convenient to assemble the array as a series of wire frames which could be stacked with various spacings, transverse offsets or rotations applied.

Representing the wire array metamaterial in the Drude model, and defining $\epsilon(\nu) = \epsilon'(\nu) - j \cdot \epsilon''(\nu)$, we have for the real and imaginary components

$$\epsilon' = 1 - \frac{\nu^2}{\nu^2 + \Gamma^2} \quad (3a)$$

and

$$\epsilon'' = \left(\frac{\nu_p}{\nu}\right)^2 \frac{\frac{\Gamma}{\nu}}{1 + \left(\frac{\Gamma}{\nu}\right)^2} \quad (3b)$$

where ν is the frequency, ν_p is the plasma frequency, and Γ the loss term. For normal incidence, the transmission through a complex dielectric slab is succinctly expressed as

$$S_{21} = \frac{(1 - \rho_0^2)e^{-(\alpha + j\beta)d}}{1 - \rho_0^2 e^{-(2\alpha + j\beta)d}} \quad (4)$$

where $\rho_0 = (1 - \sqrt{\epsilon})/(1 + \sqrt{\epsilon})$, d is the width of the array, and α and β are the attenuation coefficient and wave numbers of the propagating wave in the medium, respectively. The α and β are given by

$$\alpha(\nu) = \frac{2\pi\nu}{c} \sqrt{\frac{\epsilon'(\nu)}{2} \left\{ \sqrt{1 + \tan^2[\delta(\nu)]} - 1 \right\}} \quad (5a)$$

and

$$\beta(\nu) = \frac{2\pi\nu}{c} \sqrt{\frac{\epsilon'(\nu)}{2} \left\{ \sqrt{1 + \tan^2[\delta(\nu)]} + 1 \right\}} \quad (5b)$$

where $\tan\delta(\nu) = \epsilon''(\nu)/\epsilon'(\nu)$ is the frequency-dependent loss tangent of the material [25]. Thus S_{21}

data now can be fit with Eq. (4), and metamaterial properties extracted.

The metamaterial properties are encoded in the transition region of the S_{21} around the plasma resonance. Figure 1 shows theoretical transmission versus frequency as a function of the metamaterial characteristics. In each plot, two of three parameters of the array are fixed, with the third varying over a range encompassing representative values for our measurements.

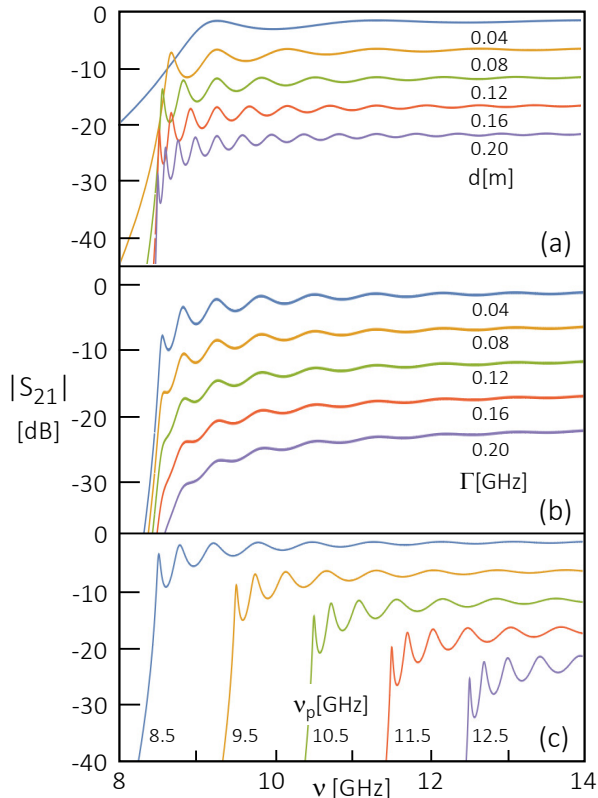


FIG. 1. Plots of $|S_{21}|$ where in each case one of the three parameters (plasma frequency, loss rate, width) of the wire array metamaterial is varied in discrete steps, leaving the other two fixed. (a) Varying the width of the slab d [m], with $\nu_p = 8.5$ GHz, $\Gamma = 0.01$ GHz. (b) Varying the loss rate Γ [GHz], with $\nu_p = 8.5$ GHz, $d = 0.12$ m. (c) Varying the plasma frequency ν_p , with $d = 0.12$ m, $\Gamma = 0.01$ GHz. For clarity, the lower curves in (a) are offset in steps of -7.5 dB, for (b) and (c) the offset of the curves are in steps of -5 dB.

EXPERIMENTAL SETUP AND MEASUREMENTS

The wire planes, 40 in total, consisted of square metal frames of 203 (254) mm inner (outer) edge length, 1.5 mm thickness, and strung with 50 μm diameter gold-ontungsten wire [28] with a wire spacing of $a = 5.88$ mm. The S_{21} measurements were carried out with standard

microwave test equipment, a vector network analyzer (VNA) [29], and matched waveguide horn antennas [30].

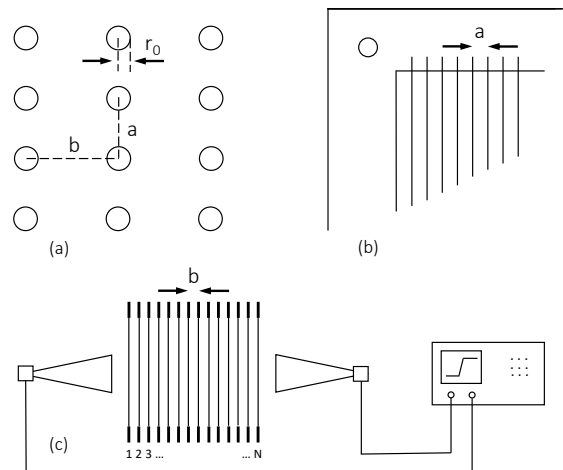


FIG. 2. (a) A rectangular wire array, with r_0 , a and b designating the radius and the spacing of the wires. (b) Detail of the construction of a single wire plane. The wires are supported by the metallic wire frame but not in electrical contact with it. (c) The geometry for the measurements of S_{21} as a function of number of wire planes, N .

The evolution of the plasmonic behavior of the metamaterial as a function of the dimension of the array was first investigated. Individual wire planes were sequentially loaded into a frame, thus constituting a rectangular array with $(a, b) = (5.88, 8.00)$ mm, and the S_{21} measured as a function of the number of wire planes, $N = 1-40$. This setup is illustrated in Figure 2. The measurements are shown in Figure 3. Even prior to detailed fitting of individual spectra to the model, the data qualitatively exhibit the expected plasmonic behavior.

Repeated measurements were taken under varying conditions to generate a complete data set for fitting S_{21} to the metamaterial properties. These included measurements of different distances between the waveguide horn antennas, and of both uncollimated and collimated geometries. To examine the onset and approach to asymptotic plasmonic response where the fitted parameters changed most rapidly, the low- N spectra ($N = 1-20$) were repeated separately with a shorter baseline between the horns, and were in good agreement with the $N = 1-40$ data. The parameters as a function of number of planes $N = 1-40$ are displayed in Figure 4. For these measurements, the waveguide antennas were spaced 40 cm apart for all N . The uncollimated data represents the intrinsic horizontal and vertical beam width of the microwave horns of $\pm 8^\circ$ at 3 dB [30]; the collimated data were taken with the same setup, but with the addition of a microwave absorbing

collimator in front of the receiver [31] with a rectangular aperture 7.5 cm (horizontal) \times 5.0 cm (vertical). In each case, both collimated and uncollimated data were collected to determine if any scattering from the metal frames was contributing to the spectra; no such evidence was seen. The comparison also confirmed that the data accurately represented strict normal incidence, as required by Eq. 4, obviating the need to average over the beam spread.

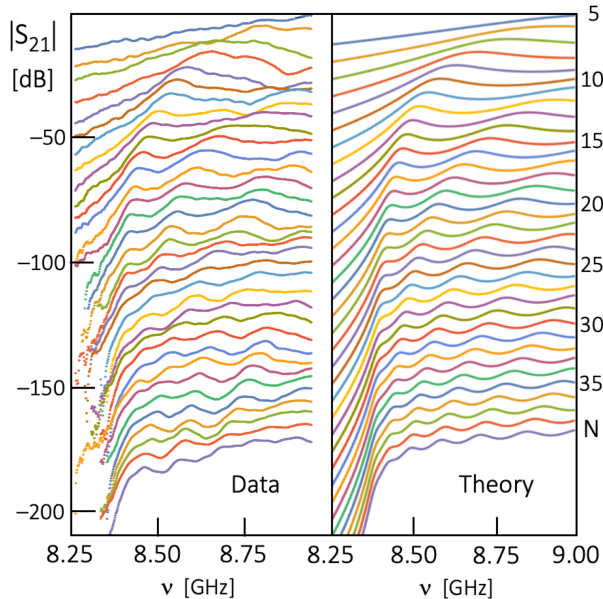


FIG. 3. Ensemble of measured and calculated S_{21} for all N ; spectra are sequentially displaced by -5 dB for clarity. The calculated spectra are all for $\nu_p = 8.35$ GHz, $\Gamma = 0.04$ GHz, and the array width $d = N \cdot b$.

Least squares fitting of the S_{21} of a frequency-dependent complex dielectric yields an effective width of the full array equal to its physical width at the few percent level (Figure 4a). It is noteworthy however that the inferred effective width $d^{\text{eff}}(N) = 0.00249 + 0.00804 \cdot N[\text{m}]$ is exactly one plane spacing greater than the physical width, $d^{\text{phy}}(N) = 0.008 \cdot (N-1)$ for all N ; equivalently it may be stated that the metamaterial effectively extends $\sim b/2$ beyond the front and back boundaries of the array.

There is already a well-defined plasma frequency even for an array of 5 periods depth, beyond which the plasma frequency increases only marginally; ν_p is within 1% of its asymptotic value, 8.37 GHz, for 10 periods, and within 0.1% by 20 periods (Figure 4b).

An important aim of this study in determining the practical utility of a wire array metamaterial in an axion haloscope was to estimate its Q under actual operating conditions, which is directly connected with loss Γ extracted from the S_{21} . The measured loss exhibits a two-component behavior (Figure 4c). The first reflects

the approach to the bulk response, $\Gamma_S \cdot \exp(-\gamma \cdot N)$, with $\Gamma_S = 1.70$ [GHz], and $\gamma = 0.47$; the second a constant term $\Gamma_B = 0.038$ [GHz], which dominates for $N > 10$ in the structure. At room temperature and with the current wire parameters, this would imply a quality factor in the bulk limit $Q = \nu_p/\Gamma \sim 220$, to be compared with a theoretical value of 260 [32]. However, a resonator of a given frequency can be designed with any choice of correlated wire radius and spacing, and for our frequency, the selection of wire radius $r_0 = 25 \mu\text{m}$ is far from optimal in terms of the quality factor. This has been studied by Balafendiev et al. [33], who finds that in the 10 GHz frequency range, the optimum Q is achieved over a broad maximum in wire radius $r_0 = O(\text{mm})$. Specifically, for a square lattice, the improvement in Q at our frequency would be a factor of $\times 17$. Finally, as the haloscope would operate at cryogenic temperatures, the Q should also improve by the ratio of the classical skin depth at 300 K to the anomalous skin depth below 4 K, a factor of $\times 5$; values of $\times 3-4$ are typical in microwave cavity dark matter experiments. Taken together, one can plausibly project unloaded quality factors $Q > 10^4$, where the actual limitation would likely be engineered features of its metallic enclosure.

Finally, two concepts for tuning a metamaterial resonator have been explored. In the first, the spacing between planes, b , has been adjusted, while keeping the spacing between wires on the plane, a , fixed (Figure 5a). Increasing the spacing from 3.1 mm to 7.6 mm results in a 40% decrease in frequency; the semianalytical treatment of Belov for the case of a rectangular unit cell ($a \neq b$) is in excellent numerical agreement with the data [25]. In the second, the plasma frequency has been measured for a parallel shift of alternate wire planes, maintaining their spacing at $b = 2.74$ mm (Figure 5b). Here, the plasma frequency undergoes a periodic oscillation with shift of the planes, increasing by 3% at $x = a/2$. COMSOL calculations of Balafendiev are in good overall agreement with the data, although 1% high [33]. However, rather than shifting the two groups of alternate planes parallel to one another, if the two groups of alternate planes are now moved with respect to one another in the normal direction, \hat{y} , thus bringing pairs of wires of neighboring planes into close proximity with one another, large changes in frequency are predicted, $\sim 30\%$ or more [33]. The current setup was not suitable to do a precision measurement to test those predictions, but will be redesigned to carry them out in the near future.

DISCUSSION

What will prove to be the most practical scheme for accurately tuning a metamaterial resonator is not yet clear. A key principle is that any global tuning motion must result in the local plasma frequency being equal at

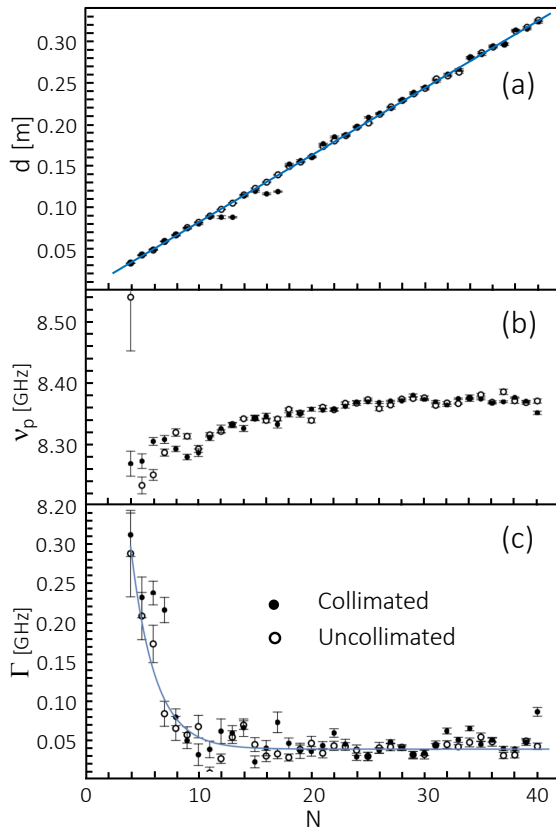


FIG. 4. Metamaterial parameters derived from the measured S_{21} as a function of the number of planes, N . (a) The effective width of the wire array metamaterial, d . (b) The plasma frequency ν_p . (c). The loss term, Γ .

every point in the entire structure, within its bandwidth $\sim 10^{-4}$. This will pose an engineering challenge for a device of a meter in dimension. Uniformly changing the spacing of planes has the advantage of keeping the individual wires relatively far apart, making for more benign tolerancing, but results in an overall change in wire density, and thus a size or shape change of the envelope of the resonator. Schemes relying on bringing pairs of wires into close proximity preserve overall shape and size of the resonator, but will stress tolerancing of wire positions. Furthermore the dynamic range in frequency is covered by an overall translation of only ~ 10 mm, posing a precision motion challenge as well. In summary, the fundamental behavior of 3-D wire array metamaterials is well understood theoretically, and the data supports its applicability as a tunable plasmonic resonator for an axion haloscope. Further study and engineering will be necessary to translate this resonator concept into a complete plasma haloscope axion search.

Acknowledgements. - This work was supported by the National Science Foundation under Grant No. 1914199. We acknowledge clarifying discussions with

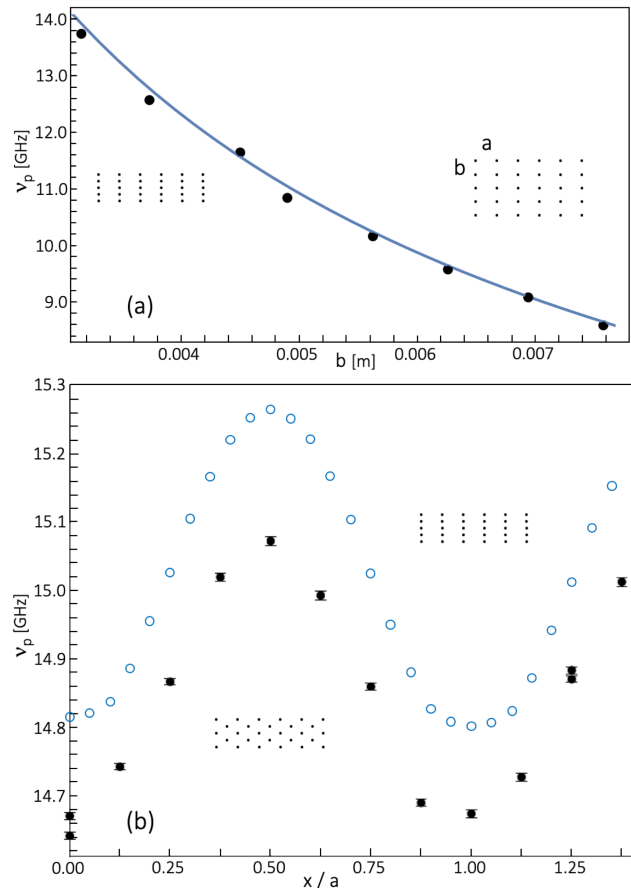


FIG. 5. Test of two tuning schemes of a 20-plane wire-array metamaterial. (a) Frequency as a function of changing one dimension of a rectangular unit cell, b , keeping a constant. Blue curve the prediction of [25]. (b) Frequency as a function of relative shift of alternate planes, maintaining b constant. Blue circles the prediction of [33].

M. Lawson, A. Millar, F. Wilczek, P. Belov, R. Balafendiev, and the entire ALPHA collaboration. We especially thank R. Balafendiev for permission to use his calculations prior to publication.

-
- [1] R.D. Peccei and H.R. Quinn, CP Conservation in the Presence of Pseudoparticles, Phys. Rev. Lett. 38, 1440 (1977).
 - [2] S. Weinberg, A New Light Boson?, Phys. Rev. Lett. 40, 223 (1978).
 - [3] F. Wilczek, Problem of Strong P and T Invariance in the Presence of Instantons, Phys. Rev. Lett. 40, 279 (1978).
 - [4] P. W. Graham and A. Scherlis, Stochastic axion scenario, Phys. Rev. D 98, 035017 (2018).
 - [5] F. Takahashi, W. Yin, and A. H. Guth, QCD axion window and low-scale inflation, Phys. Rev. D 98, 015042 (2018).

- [6] M. Buschmann, J. W. Foster, and B. R. Safdi, Early-Universe Simulations of the Cosmological Axion, *Phys. Rev. Lett.* 124, 161103 (2020).
- [7] M. Buschmann, J. W. Foster, A. Hook, A. Peterson, D. E. Willcox, W. Zhang, and B. R. Safdi, Dark matter from axion strings with adaptive mesh refinement, *Nat. Commun.* 13, 1049 (2022).
- [8] P. Sikivie, Experimental tests of the “invisible” axion, *Phys. Rev. Lett.* 51, 1415 (1983).
- [9] P. Sikivie, Detection rates for invisible axion searches, *Phys. Rev. D* 32, 2988 (1985).
- [10] J. Liu, K. Dona, G. Hoshino, S. Knirck, N. Kurinsky, M. Malaker, D. Miller, A. Sonnenschein, P. Barry, K.K. Berggren et al., Broadband Solenoidal Haloscope for terahertz axion detection, arXiv:2111.12103v1.
- [11] C. Lee, the MADMAX collaboration, Status of the MADMAX Experiment, in: G. Carosi, G. Rybka [eds] *Microwave Cavities and Detectors for Axion Research*, Springer Proceedings in Physics. vol. 245. Springer, Cham.
- [12] B. M. Brubaker, L. Zhong, Y. V. Gurevich, S. B. Cahn, S.K. Lamoreaux, M. Simanovskaia, J. R. Root, S. M. Lewis, S. Al Kenany, K. M. Backes, et al., First Results from a Microwave Cavity Axion Search at 24 μeV , *Phys. Rev. Lett.* 118, 061302 (2017).
- [13] C. Bartram, T. Braine, E. Burns, R. Cervantes, N. Crisosto, N. Du, H. Korandla, G. Leum, P. Mohapatra, T. Nitta, et al., Search for Invisible Axion Dark Matter in the 3.3–4.2 μeV Mass Range, *Phys. Rev. Lett.* 127, 261803 (2021).
- [14] S. Lee, S. Ahn, J. Choi, B. R. Ko, and Y. K. Semertzidis, Axion Dark Matter Search around 6.7 μeV , *Phys. Rev. Lett.* 124, 101802 (2020).
- [15] K. M. Backes, D. A. Palken, S. A. Kenany, B. M. Brubaker, S. B. Cahn, A. Droster, G. C. Hilton, S. Ghosh, H. Jackson, S. K. Lamoreaux, et al., A quantum enhanced search for dark matter axions, *Nature* 590, 238 (2021).
- [16] K. van Bibber, K. Lehnert and A. Chou, Putting the Squeeze on the Axion, *Phys. Today*, June, 2019.
- [17] P. Sikivie, N. Sullivan and D.B. Tanner, Proposal for Axion Dark Matter Detection using an LC Circuit, *Phys. Rev. Lett.* 112, 131301 (2014).
- [18] S. Chaudhuri, P. W. Graham, K. Irwin, J. Mardon, S. Rajendran, and Y. Zhao, A Radio for Hidden Photon Dark Matter, *Phys. Rev. D* 92, 075012 (2015). (While originally proposed as a hidden photon search, as envisioned from the beginning, the experiment becomes sensitive to the axion as well, just with the addition of a magnet and minor changes of configuration.)
- [19] C. P. Salemi, J. W. Foster, J. L. Ouellet, A. Gavin, K. M. W. Pappas, S. Cheng, K. A. Richardson, R. Henning, Y. Kahn, R. Nguyen, et al., Search for Low-Mass Axion Dark Matter with ABRACADABRA-10 cm, *Phys. Rev. Lett.* 127, 081801 (2021).
- [20] M. Silva-Feaver, S. Chaudhuri, H. M. Cho, C. Dawson, P. Graham, K. D. Irwin, S. Kuenstner, D. Li, J. Mardon, H. Moseley, and R. Mule, *IEEE Trans. on Appl. Superconductivity* 27, 1 (2016).
- [21] M. Simanovskaia, A. Droster, H. Jackson, I. Urdinaran, and K. van Bibber, A Symmetric Multi-rod Tunable Microwave Cavity for the HAYSTAC Dark Matter Axion Search, *Rev. Sci. Instr.* 92, 033305 (2021).
- [22] S. D. Kinion, First results from a multiple microwave cavity search for dark matter axions, Ph.D. thesis, University of California Davis (2001).
- [23] M. Lawson, A. J. Millar, M. Pancaldi, E. Vitagliano, and F. Wilczek, Tunable Axion Plasma Haloscope, *Phys. Rev. Lett.* 123, 141802 (2019).
- [24] J. B. Pendry, A. J. Holden, D. J. Robbins, and W. J. Stewart, Low frequency plasmons in thin-wire structures, *J. Phys. Condens. Matter* 10, 4785 (1998).
- [25] P. A. Belov, R. Marqués, S. I. Maslovski, I. S. Nefedov, M. Silveirinha, C. R. Simovski, and S. A. Tretyakov, Strong spatial dispersion in wire media in the very large wavelength limit, *Phys. Rev. B* 67, 113103 (2003).
- [26] P. Gay-Balmaz, C. Maccio, and O. J. F. Martin, Microwire arrays with plasmonic response at microwave frequencies, *Appl. Phys. Lett.* 81, 2896 (2002).
- [27] A. Yahalom, Y. Pinhasi, E. Shifman, and S. Petnev, Transmission through Single and Multiple Layers in the 3–10 GHz Band and the Implications for Communications of Frequency Varying Material Dielectric Constants, *WSEAS Transactions on Communications* 9, 759 (2010).
- [28] Luma Metall AB, Kalmar, Sweden, <https://luma-metall.com/>.
- [29] Keysight Technologies, 4-port VNA, E5071C, Santa Rosa, California, <https://www.keysight.com/us/en/home.html>.
- [30] Pasternak Enterprises Electronics, WR-90 series, PE9856B-20, Irvine, California, <https://www.pasternack.com/>.
- [31] Laird Co., Eccosorb OCF series, <https://laird.com/>.
- [32] R. Balafendiev, P. Belov, C. Simovski, and A. J. Millar, Wire medium filled metallic resonators, arXiv:2203.10083v1.
- [33] R. Balafendiev, private communication (2022).